

Fine-tuned Circuit Representation of Human Vessels through Reinforcement Learning: A Novel Digital Twin Approach for Hemodynamics

Jorge Torres Gomez
TU Berlin, Germany
torres-gomez@ccs-labs.org

Jorge Luis González Rios
University of Luxembourg, Luxembourg
jorge.gonzalez@uni.lu

Nicolai Spicher
University of Göttingen, Germany
nicolai.spicher@ieee.org

Falko Dressler
TU Berlin, Germany
dressler@ccs-labs.org

ABSTRACT

The modeling of human vessel hemodynamics targets various benefits in health care applications. Subject-specific models of vessels allow the accurate prediction of pressure and flow, thus, enabling the study of individuals' responses to medical treatment. Instead of developing a model for a standard person, this paper features a design for the human circulatory system (HCS) accounting for the specific physiological parameters of an individual. We report using a reinforcement learning (RL) model for customary vessel parameters when training with subject-specific pressure and flow waveforms. We use an equivalent electric-circuit model for the human arteries and adjust the values of resistors, inductors, and capacitors in combination with reinforcement learning (RL). The conceived model stems as a digital twin replicating specific subjects. The reinforcement learning (RL) method predicts the vessel length and radius with an error of less than 10 % and fits pressure waveforms with a similarity higher than 94 %.

CCS CONCEPTS

• **Applied computing** → **Health informatics**; • **Hardware** → **Biology-related information processing**.

KEYWORDS

Human Circulatory System, Electric Circuit Simulator, Blood Pressure, Reinforcement Learning

ACM Reference Format:

Jorge Torres Gomez, Nicolai Spicher, Jorge Luis González Rios, and Falko Dressler. 2023. Fine-tuned Circuit Representation of Human Vessels through Reinforcement Learning: A Novel Digital Twin Approach for Hemodynamics. In *The 10th ACM International Conference on Nanoscale Computing and Communication (NANOCOM '23)*, September 20–22, 2023, Coventry, United Kingdom. ACM, New York, NY, USA, 7 pages. <https://doi.org/10.1145/3576781.3608717>

Permission to make digital or hard copies of all or part of this work for personal or classroom use is granted without fee provided that copies are not made or distributed for profit or commercial advantage and that copies bear this notice and the full citation on the first page. Copyrights for components of this work owned by others than the author(s) must be honored. Abstracting with credit is permitted. To copy otherwise, or republish, to post on servers or to redistribute to lists, requires prior specific permission and/or a fee. Request permissions from permissions@acm.org.
NANOCOM '23, September 20–22, 2023, Coventry, United Kingdom

© 2023 Copyright held by the owner/author(s). Publication rights licensed to ACM.
ACM ISBN 979-8-4007-0034-7/23/09...\$15.00
<https://doi.org/10.1145/3576781.3608717>

1 INTRODUCTION

According to the World Health Organization, more than one billion adults worldwide suffer from high blood pressure levels (hypertension), with approximately half of them not being aware of their condition and not being treated adequately.¹ Their treatment is one of the global endeavors so as to reduce the prevalence of hypertension by 33 % until 2030. Targeting this aim requires intense applied research on modeling the human circulatory system (HCS) as well as hemodynamics, the research area dealing with the dynamics of the blood flowing within the circulatory system. Modeling hemodynamics in vessels pave the way for accurate prediction of pressure and flow in the arteries as well as the individual response to medical treatment [3].

Targeting real-world clinical data, a digital twin (DT) replica for subject-specific hemodynamics will allow customized medical treatment for improved healthcare [4]. Modeling the HCS, backbone studies of translational research model the fluid-dynamics effects in vessels, like laminar flow or turbulence, through the numerical evaluation of Navier-Stokes equations for fluids as 3-D models [5]. The 0-D models, with fewer details and less computational complexity, translate vessels' physiology to electric circuit parameters as resistors, inductors and capacitors [12]. Using the electric circuit representation, the voltage is translated to the variable time evolution of pressure and the current to blood flow. Resistors represent the resistance to the blood, inductors the blood inertia, and capacitors vessels compliance. The 0-D models significantly reduce computational resources allowing to simulate a complete representation of the main arteries, capillaries, and veins in the body (see for instance [12, Fig. 4.0.1 pag. 70]).

Various works tune 0-D models parameters to clinical data with the Windkessel model, fitting the systemic circulation for particular subjects. Research is reported through manual tuning [11], or automatically using numerical solutions [13, 15] and predictors like the Kalman filter [9]. Although these contributions fit parameters to clinical data for particular subjects, they are limited to reproducing the pressure and flow but only for a single major artery (Root Aorta). The Windkessel model represents the whole systemic circulation missing to represent details on other major arteries in the body like femoral, ulnaris, and carotid.

¹World Health Organization, Hypertension Factsheet. <https://www.who.int/news-room/fact-sheets/detail/hypertension>, Accessed: 2023-03-29

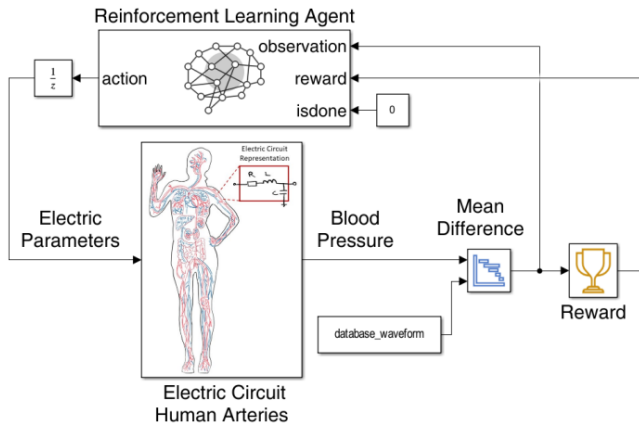


Figure 1: Connection of agent (reinforcement learning) and the environment (human circulatory system).

Filling this gap, we aim to customize electric-circuit models for a complete representation of the major arteries. We propose a novel methodology for applying the concept of DT to hemodynamics using reinforcement learning (RL). An RL agent is applied to learn the best-fitting electric parameters for reproducing blood pressure waveforms of individual subjects with the original waveforms stemming from publicly-available virtual datasets. As Fig. 1 depicts, the Agent will automatically modify the electric circuit parameters (Resistor, Inductor, Capacitor), using the mean difference between the predicted blood pressure and the original waveform from the database. Besides, with the RL agent, the model is also flexible with the dynamic of human activities, i.e., while doing sport in a very active regime. Overall, this solution resembles a DT model, popularly reported in healthcare applications [1, 3], while accounting for the physiological parameters of a particular subject.

As a resulting main contribution, we provide an expedited model for the HCS, which automatically fits the pressure levels to a particular subject. Besides, such a model lets indirectly estimate vessels’ physiological parameters concerning their length, radius, and thickness from pressure waveforms (non-invasive means). As a particular distinction, the trained RL model might also be used to estimate these parameters in real-time for clinical studies. Elaborating on these contributions, the remainder of this paper is structured as follows. The detailed description of the model is outlined in Section 2 building on the electric circuit design proposed in the previous work [14] and extending it by integration of the RL model. The resulting estimated parameters and their pressure resemblance to database waveforms are highlighted in Section 3 and concluded in Section 4.

2 DIGITAL TWIN MODEL: REINFORCEMENT LEARNING – ELECTRIC CIRCUIT

The equivalent DT is achieved by integrating the RL model with the electric circuit design. The design entails four main blocks, as depicted in Fig. 1, namely

- Environment: electric circuit design for the HCS simulating the blood pressure,
- Agent block: to run RL as a Deep Q-Network (DQN),

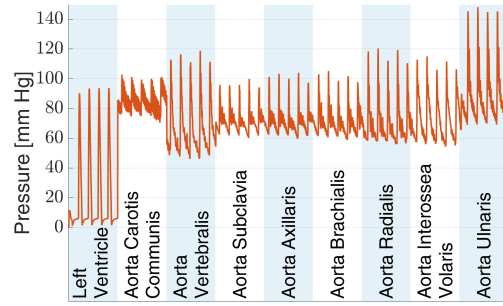


Figure 2: Simulated blood pressure in arms of a simulated healthy subject with a heart rate of 75 beats/min.

- Mean difference block: to produce the agent’s observations,
- Reward block: to score the actions the agent made.

This way, the RL agent will actuate on the electric circuit parameters aiming to minimize the difference between the blood pressure on the HCS-circuit and the given database waveform. The following subsections outline more details on each different block.

2.1 Dataset

We use a synthetic dataset with the pressure values to train the Agent and evaluate the accuracy of the proposed method. We use the design of Noordergraaf et al. [8], which comprises a 0-D model for the human vessels as an electric circuit. The electric circuit design provides pressure waveforms and flows for 128 vessel segments in the arteries as well as the length and radius per vessel segment (see [8, Table 1]).² This model corresponds to an average healthy subject (height: 175 cm, mass: 75 kg heart rate: 75 beats/min).

To illustrate some pressure waveforms, Fig. 2 plots the pressure in the arms. The waveforms illustrate a typical behavior for the blood pressure of healthy subjects with the largest oscillation being in the left ventricle, and its elongation is reduced in the arms and legs’ arteries (cf. [6, Fig. 14-2 pag. 172]). We also remark on the increased amplitude in the large arteries (e.g., Aorta Carotis) compared to the left ventricle as typical behavior of the blood pressure in vessels. We use these waveforms for training the RL agent. Further details on the electric circuit design are presented in the next subsection as we use this model for the agent’s environment.

2.2 Electric Circuit Design

The complete circuit is implemented in Simulink/Matlab® Version 2022b using resistors, inductors, capacitors, and diodes from the Simscape library. The HCS-circuit implementation follows the previous work in [14] with the original design of Noordergraaf et al. [8]. It is conceived as the cascade connection of RLC circuit blocks (representing the arteries) and terminated with resistors (representing the capillaries). All the arteries are modeled with the same RLC topology (L-inverted) and terminated with the resistors. The design¹ is illustrated in Fig. 3 for the center body (Aorta Ascendens, or Thorax Aorta) with terminator resistors R₆₄ and R₆₅ for the capillaries (we follow the concepts in [8]).

²accessible online: Electric circuit representation of the human arteries. <https://www.mathworks.com/matlabcentral/fileexchange/109935-electric-circuit-representation-of-the-human-arteries>

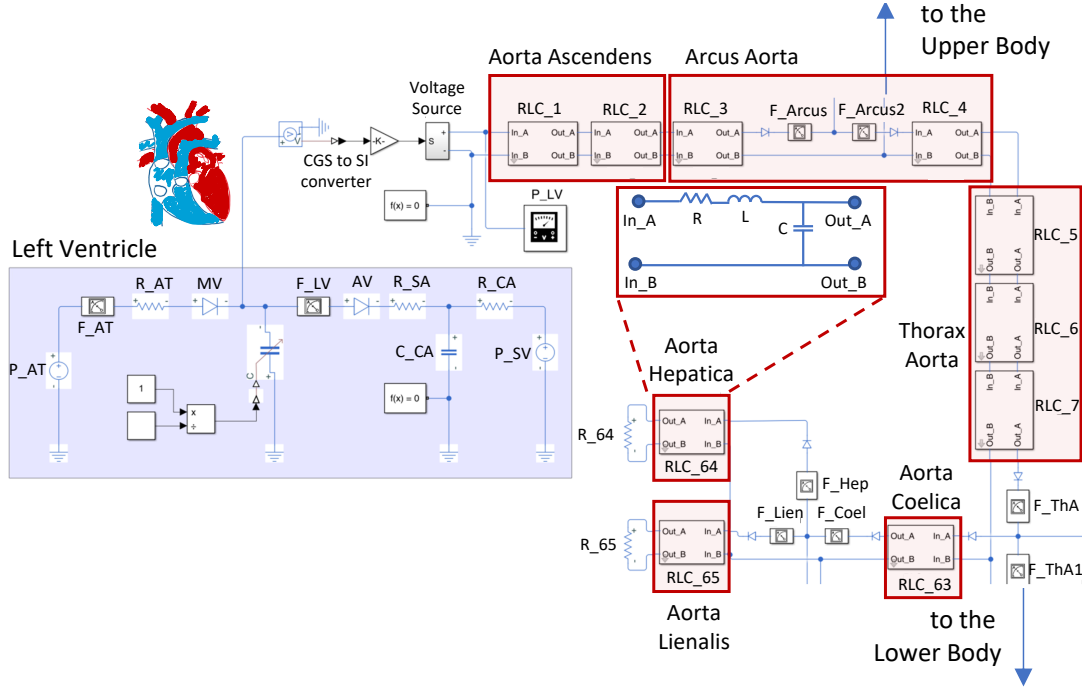


Figure 3: Electric circuit design of the human arteries

On each block, the resistor, inductor, and capacitor model the physiologic parameters of blood and the vessel segment. The electric circuit models the input and output pressures (P) and flows (Q) with a system of first-order differential equation as [7, Eq. (10)]

$$\begin{cases} C \frac{dP_{in}}{dt} + Q_{out} - Q_{in} = 0 \\ L \frac{dQ_{out}}{dt} + P_{out} - P_{in} + RQ_{out} = 0 \end{cases} \quad (1)$$

The resistor accounts for the resistance to the blood flow with the blood viscosity (μ) as [16]

$$R = \frac{8\mu}{A^2} l_v, \quad (2)$$

where l_v is the vessel length, $A = \pi r_v^2$ is sectional vessel area, and r_v the vessel radius. The inductor models the inertia of the blood with the blood density (ρ) as

$$L = \frac{\rho}{A} l_v. \quad (3)$$

The resistor and the inductor increase with the vessel length and decrease with the vessel's radius. The capacitor accounts for the compliance of the vessel with the Young Modulus (E) as

$$C = \frac{3A}{2E} \frac{r_v l_v}{h_v}, \quad (4)$$

where h_v denotes the vessel thickness.

In addition, we included the circuit representation of the left ventricle in the heart following the design in [12, Fig. 4.2.1 pag. 79]. This block models the heart pressure waveform at the left ventricle using a variable capacitor and the voltage sources P_{AT} for the atrial pressure and P_{SV} for the venous pressure. The design also includes resistors and diodes to control the amount and direction

of the blood flow. The circuit reproduces the standard waveform for the ventricular pressure, volume, and cardiac cycle as depicted in Fig. 4. A voltage-controlled source connects the heart design to the arteries without producing any additional circuit load in the interface, see Fig. 3.

2.3 Integrating the Reinforcement Learning model and the Electric Circuit

We combine the Agent with the circuit model by defining the generation of the blood pressure waveforms as an optimization problem. We do this integration using as environment the complete circuit design in Fig. 3 to evaluate specific vessel segments. In both cases, the Agent modifies the parameters of the electrical circuit (Resistor, Inductor, Capacitor), attempting to generate a pressure curve similar to the ground truth waveform. Depending on the similarity between generated and ground truth waveforms, the Agent is rewarded for predicting the optimal (R,L,C) combination that fits best to the ground truth waveform in the database. An example is illustrated in Fig. 5a, where the RL model reproduces a waveform quite similar to the Noordergraf waveform with a correlation coefficient close to one (see Fig. 5b). In this way, the RL model attempts to fit the differential equations system in Eq. (1) while tuning its parameter to reproduce the database's waveform. Further details on integrating the RL model to the circuit design are given in the following subsections.

Agent Actions: The agent's actions are directly mapped to the values of resistors, inductors, and capacitors in the electric circuit design. On a given block in the circuit in Fig. 3, we replace the resistor with a potentiometer and the inductor and capacitor with a voltage-controlled inductor and capacitor, respectively, as sketched

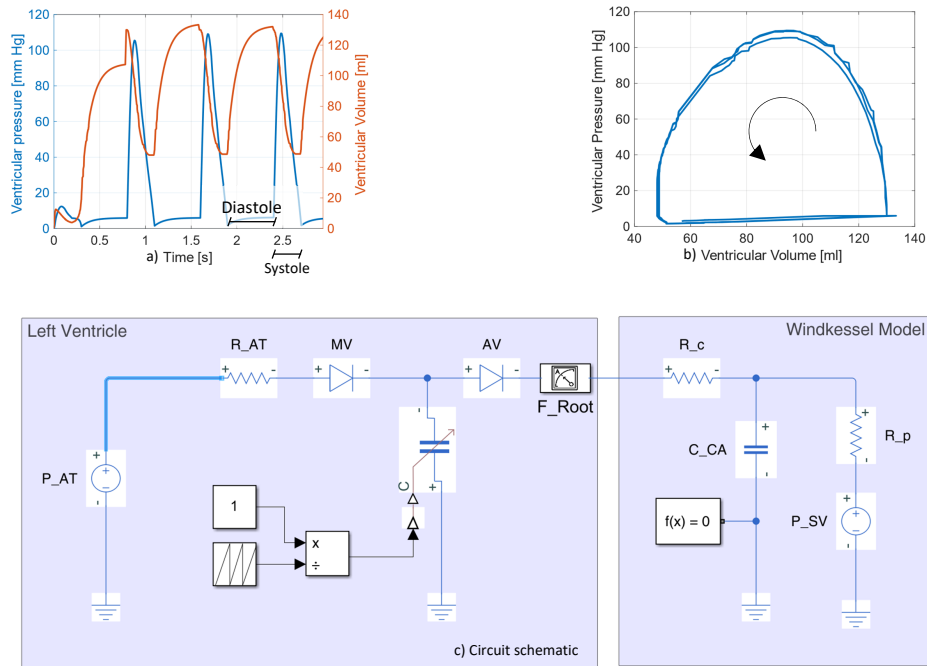
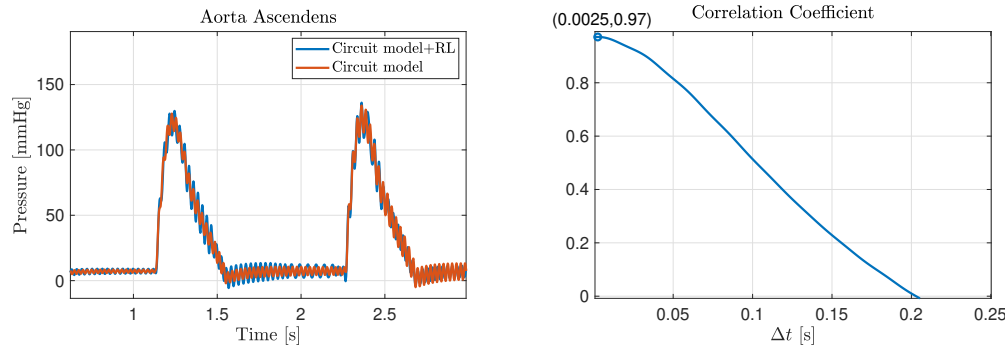


Figure 4: Electric circuit for the heart [12] and output blood flow, including the pressure and cardiac cycle in the left ventricle.



(a) Comparative plot between the ground truth signal (orange) and the generated signal (blue). (b) Correlation coefficient of the two waveforms.

Figure 5: Blood pressure and correlation coefficient in the Aorta Ascendens.

in Fig. 6. This way, the agent will control the nominal values for the three-element circuit.

In this solution we interconnect the agent to a single block attempting to reduce the computational complexity of training the Agent. For instance, if we want to replicate the pressure in the Aorta Hepatica as given in the database, the electric circuit will output the voltage on the resistor R₆₄, and the agent will be connected to the RLC₆₄ block in Fig. 3.

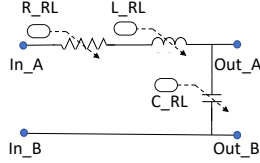
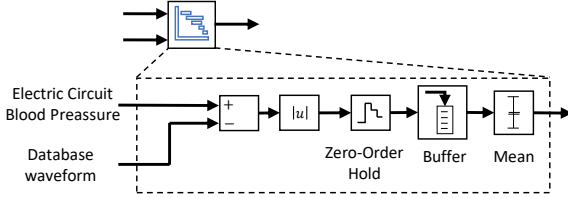
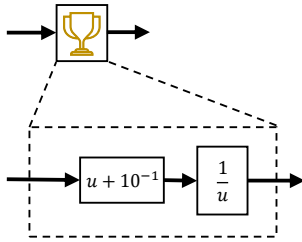
Connecting the agent to more blocks implies an action space (combined RLC ternary values) exponentially growing with the total of blocks. To illustrate, let's assume the resistor, inductor, and capacitor values range in three sets of N elements each, yielding a total combination of N^3 possible ternaries. Besides, with an arbitrary total of blocks B , the action space increases exponentially

as N^{3B} , as each block also comprises an RLC ternary set. This exponential increase in the action space will eventually be prohibitive to scale this solution; however, we will show promising results in Section 3 when connecting the agent to just a single one.

Agent Observation: When connecting the Agent's action to the circuit, we define the observation as the closeness to the blood pressure we want to reproduce. We implement this observation as the mean difference between the two waveforms in the Mean Difference block (see Fig. 1), as depicted in Fig. 7. The signal from the database is subtracted from the input signal (electric circuit's output), and its absolute value is sampled with the Zero-Order Hold block to evaluate the difference in the discrete domain. Next, the Buffer block outputs a sequence allowing us to evaluate the difference's mean along the buffer length (as a moving average window). In this design, we assume a buffer length so as to capture

Table 1: Electric and physiologic vessel parameters predicted by the RL model (relative errors to the baseline model in [8]).

Vessel	R [Ω]	L [H]	C [μF]	Length [cm]	Length relative error	Radius [cm]	Radius relative error	Thickness [mm]	Thickness relative error
Aorta Ascendens	0.052	0.34	82	3.2	9.9 %	1.3	5.1 %	0.9776	51 %
Carotis Aorta	22	8.1	5.3	17	6.6 %	0.35	4.7 %	1.57	34.4 %
Aorta Radialis	50	15	57	20	0.7 %	0.15	1.9 %	1.45	35.6 %
Aorta Femoralis	5.8	6.8	4.1	25	10 %	0.33	2.9 %	2.55	65.2 %


Figure 6: Electric circuit design integrating the agent and the circuit elements.

Figure 7: Block Diagram for the Mean Difference block.

Figure 8: Reward block diagram.

one cardiac cycle, and the difference is sampled with the sampling rate of the original circuit design as 1 ms.

Agent Reward: The reward is proportionally inverted to the difference between the circuit and database waveforms. In this way, Agent’s observation for low values is rewarded higher. As depicted in Fig. 8, the input sequence is inverted after being biased by the amount 10^{-1} . This bias is used to avoid the division by zero and also sets a maximum reward of 10 units.

Agent Model: For the Agent’s model, we implemented a DQN agent as the RL method. DQN is a variant of Q-learning and entails a recurrent neural network (RNN) avoiding storing large Q-tables instead. This model allows critics to estimate future rewards according to their current actions following the epsilon-greedy policy. This policy avoids local minima selecting a random action with probability $\epsilon = 0.9$, or a greedy action with probability $(1 - \epsilon)$, when looking for the highest value function.

Agent Training: The training is performed with the waveforms from the original electric circuit design illustrated in Fig. 3 [8] (No-ordergraaf model). We train the Agent so as to mimic pressure waveforms at specific vessel segments, one at a time. During training, the critic is updated using randomly stored past experiences of a total of 64 samples. Updates happen within a period of one cardiac cycle, according to the length of the observation window. We use a single episode of 100 sec (more than 80 periods of the cardiac cycle), as there is any random initial condition in the experiment.

3 RESULTS

Using the introduced integration between the Agent and the electric circuit model we highlight two main results: i) The similarity of the produced pressure waveform with the ground truth waveforms and ii) the accuracy on predicting physiological parameters like vessel length and radius at different arteries. In addition, we illustrate the model applicability predict the speed of the blood flow in the vessel and monitor the cardiac output when using the Windkessel scheme.

3.1 Similarity of Pressure Waveforms

For the similarity between pressure waveforms, we plot the ground truth and derived pressures while computing the correlation coefficient between the two as a metric of similarity. Similar waveforms will present a correlation coefficient close to one [10]. Figures 9 to 11 illustrate the closeness of the RL method with the original circuit design waveform in a) coming from [8]. The different artery segments are selected in the limbs (Radialis and Aorta) and the Head (Carotis). In the three cases the correlation coefficient results larger than 0.9 (see the plots in b)), providing an accurate correspondence to the original circuit model from Noordergraaf et al. [8].

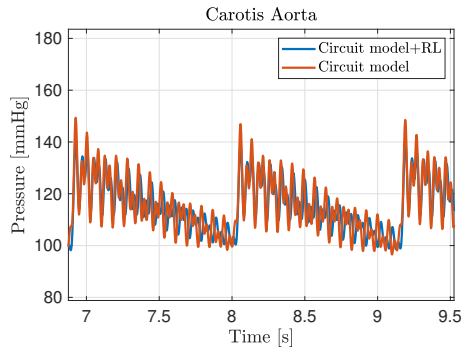
3.2 Prediction of Vessel Parameters

We estimate the predicted length (l_v), radius (r_v) and elasticity (E) of the vessel segment using the predicted values for R , L , and C by the RL model. Using Equations (2) and (3) we solve for the parameters

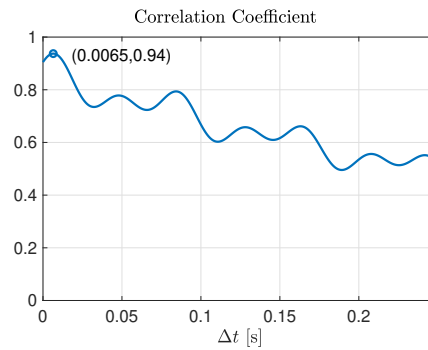
$$l_v = \frac{8\pi\mu L^2}{\rho^2 R}, \quad r_v = \sqrt{\frac{8\pi\mu L}{\rho R}}, \quad (5)$$

and replacing these results in Eq. (4) we estimate the vessel’s thickness as

$$h_v = \frac{3\pi}{2EC} r_v^3 l_v. \quad (6)$$

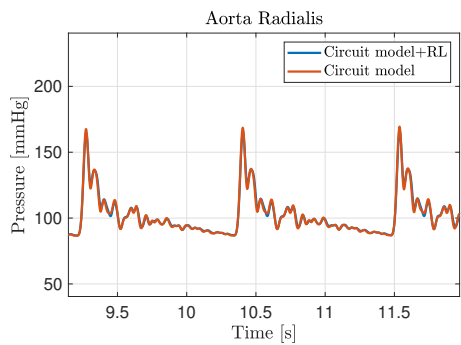


(a) Comparative plot of the ground truth signal (orange) and the generated signal (blue).

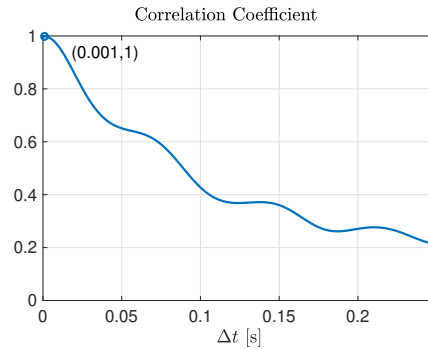


(b) Correlation coefficient of the two waveforms.

Figure 9: Blood pressure and correlation coefficient in the Carotis Aorta.

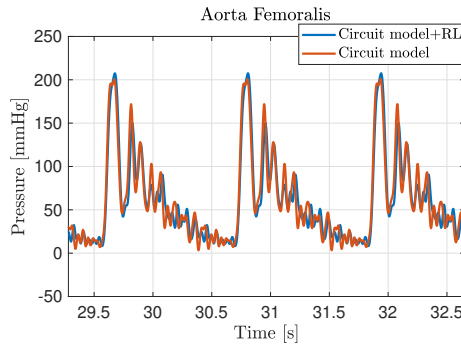


(a) Comparative plot of the ground truth signal (orange) and the generated signal (blue).

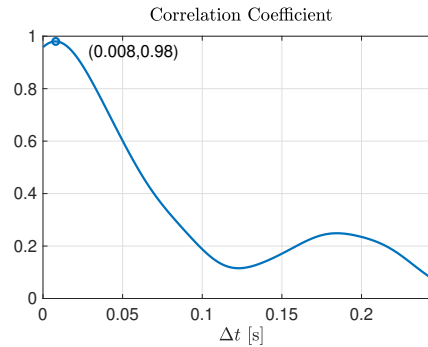


(b) Correlation coefficient of the two waveforms.

Figure 10: Blood pressure and correlation coefficient in the Aorta Radialis.



(a) Comparative plot of the ground truth signal (orange) and the generated signal (blue).



(b) Correlation coefficient of the two waveforms.

Figure 11: Blood pressure and correlation coefficient in the Aorta Femoralis.

As for the blood viscosity we consider $\mu = 3 \times 10^{-2}$ P and blood density as $\rho = 1.05 \text{ g/cm}^3$ in the centimetre–gram–second system (CGS) unit [16].³

Using these relations, we get the length, radius, and thickness per vessel segment with the predicted RLC values. To illustrate, the RL model outputs the value of the three elements, as depicted in

³We use the CGS units as the original work from Noordergraaf et al. [8] computes the values for resistors, inductors, and capacitors using this system.

Fig. 12 for the Aorta Ascendens, and using these, we get the vessel parameters as listed in Table 1. According to the table, the relative error results in less than 10 % for the vessel length and radius, except for the thickness, where the error is higher. In the case of the thickness, which depends on the capacitor (see Eq. (4)), we presume that adjusting the pressure waveform has little sensitivity with the capacitor value. Thereby a good fit with the pressure waveform is achieved in a range of capacitor values.

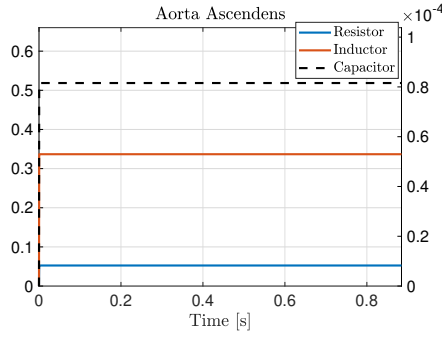


Figure 12: RL prediction for the Electric circuit parameters in the Aorta Ascendens: Resistor, Inductor, and Capacitor in the Aorta Radialis.

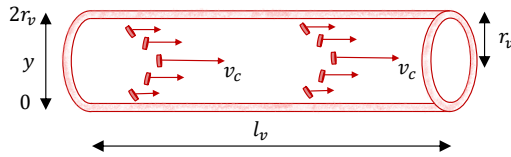


Figure 13: Representation of a vessel segment.

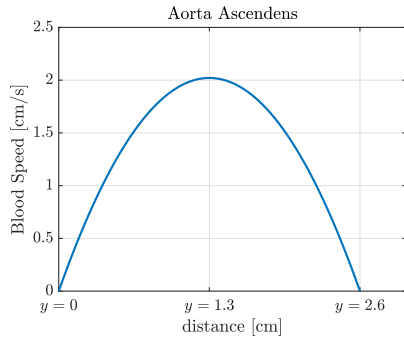


Figure 14: Estimated profile for the blood speed in the Aorta Ascendens.

3.3 Predicting Blood Speed in Arteries

Using the predicted values for the radius and length allows also estimate the flow inside the vessel. In the vessels the blood speed follows a parabolic profile along the diameter, represented with y in Fig. 13). The blood speed $v(y)$, due to a difference in pressure along the vessel segment is [2, Eq. 4.9 pag. 54]

$$v(y) = \frac{v_c}{r_v^2} (2r_v y - y^2), \quad y \in [0, 2r_v], \quad (7)$$

where v_c is the maximum speed at the vessel center as

$$v_c = \frac{\Delta P r_v^2}{2\mu l_v}. \quad (8)$$

Using the predicted l_v and r_v we can estimate the blood flow dynamics with Equations (7) and (8). To illustrate, Fig. 14 plots the blood speed with y in the Aorta Ascendens using the parameters listed in Table 1. With a similar procedure, the profile can also be estimated for other vessel segments.

4 CONCLUSION

This paper evidences a method to estimate vessel physiologic parameters from pressure waveforms. The method fits the model output pressure to the database waveform while tuning the vessel length, radius, and thickness. We use RL to fit the model and learn the subject-specific parameters, in this way devising a digital twin for the main arteries. Although improvements are needed to estimate the thickness, the model achieved estimation errors that resulted in less than 10 % for the vessel length and radius. As future work we will implement more accurate models, like different policies and reward functions, to further reduce the estimation errors.

ACKNOWLEDGMENT

Reported research was supported by project NaBoCom funded by German Research Foundation (DFG) under grant DR 639/21-1, and by the Luxembourg National Research Fund CORE Project ARMMONY (C21/IS/16352790).

REFERENCES

- [1] Emily Anthes. 2023. Could the Next Blockbuster Drug Be Lab-Rat Free? *The New York Times* (March 2023).
- [2] Howard C. Berg. 1993. *Random Walks in Biology*. Princeton University Press.
- [3] Genevieve Coorey, Gemma A. Figtree, David F. Fletcher, Victoria J. Snelson, Stephen Thomas Vernon, David Winlaw, Stuart M. Grieve, Alistair McEwan, Jean Yee Hwa Yang, Pierre Qian, Kieran O'Brien, Jessica Orchard, Jinman Kim, Sanjay Patel, and Julie Redfern. 2022. The health digital twin to tackle cardiovascular disease—a review of an emerging interdisciplinary field. *npj Digital Medicine* 5, 1 (Aug. 2022). <https://doi.org/10.1038/s41746-022-00640-7>
- [4] Hadeel Elayan, Moayad Aloqaily, and Mohsen Guizani. 2021. Digital Twin for Intelligent Context-Aware IoT Healthcare Systems. *IEEE Internet of Things Journal* 8, 23 (Dec. 2021), 16749–16757. <https://doi.org/10.1109/jiot.2021.3051158>
- [5] Luca Formaggia, Alfio Quarteroni, and Alessandro Veneziani (Eds.). 2009. *Cardiovascular Mathematics: Modeling and simulation of the circulatory system*. Springer-Verlag, Berlin, Germany. <https://doi.org/10.1007/978-88-470-1152-6>
- [6] Arthur C. Guyton and Michael. E. Hall. 2015. *Guyton and Hall Textbook of Medical Physiology* (14 ed.). Elsevier.
- [7] Vuk Milišić and Alfio Quarteroni. 2004. Analysis of lumped parameter models for blood flow simulations and their relation with 1D models. *ESAIM: Mathematical Modelling and Numerical Analysis* 38, 4 (July 2004), 613–632. <https://doi.org/10.1051/m2an:2004036>
- [8] Abraham Noordergraaf, Pieter D. Verdouw, and Herman B.K. Boom. 1963. The use of an analog computer in a circulation model. *Progress in Cardiovascular Diseases* 5, 5 (March 1963), 419–439. [https://doi.org/10.1016/s0033-0620\(63\)80009-2](https://doi.org/10.1016/s0033-0620(63)80009-2)
- [9] S. Pant, B. Fabrèges, J-F. Gerbeau, and I. E. Vignon-Clementel. 2014. A methodological paradigm for patient-specific multi-scale CFD simulations: from clinical measurements to parameter estimates for individual analysis. *International Journal for Numerical Methods in Biomedical Engineering* 30, 12 (Nov. 2014), 1614–1648. <https://doi.org/10.1002/cnm.2692>
- [10] Peyton Peebles Z. 1987. *Probability, random variables, and random signal principles*. McGraw-Hill, Inc. 352 pages.
- [11] Giancarlo Pennati, Raffaele Corsini, Daria Cosentino, Tain-Yen Hsia, Vincenzo S. Luisi, Gabriele Dubini, and Francesco Migliavacca. 2011. Boundary conditions of patient-specific fluid dynamics modelling of capovulmonary connections: possible adaptation of pulmonary resistances results in a critical issue for a virtual surgical planning. *Interface Focus* 1, 3 (March 2011), 297–307. <https://doi.org/10.1098/rsfs.2010.0021>
- [12] Vincent C. Rideout. 1991. *Mathematical and Computer Modeling of Physiological Systems*. Prentice Hall, Upper Saddle River, NJ.
- [13] Ryan L. Spilker and Charles A. Taylor. 2010. Tuning Multidomain Hemodynamic Simulations to Match Physiological Measurements. *Annals of Biomedical Engineering* 38, 8 (March 2010), 2635–2648. <https://doi.org/10.1007/s10439-010-0011-9>
- [14] Jorge Torres Gómez, Jorge Luis González Rios, and Falko Dressler. 2022. Nanosensor Location in the Human Circulatory System based on Electric Circuit Representation of Vessels. In *ACM NANOCOM 2022*. ACM, Barcelona, Spain, 1–7. <https://doi.org/10.1145/3558583.3558818>
- [15] G. Troianowski, C. A. Taylor, J. A. Feinstein, and I. E. Vignon-Clementel. 2011. Three-Dimensional Simulations in Glenn Patients: Clinically Based Boundary Conditions, Hemodynamic Results and Sensitivity to Input Data. *Journal of Biomechanical Engineering* 133, 11 (Nov. 2011). <https://doi.org/10.1115/1.4005377>
- [16] Nicolaas Westerhof, Frederik Bosman, Cornelis J. De Vries, and Abraham Noordergraaf. 1969. Analog studies of the human systemic arterial tree. *Journal of Biomechanics* 2, 2 (May 1969), 121–143. [https://doi.org/10.1016/0021-9290\(69\)90024-4](https://doi.org/10.1016/0021-9290(69)90024-4)